Research Proposal for the Biophysics Oral Exam
of
Weiwei Gu

June 11, 1999

Table of contents

A. Scientific Questions and Specific Aims 2

B. Biological Systems 2

(I) Hydrogenase 2

(II) Carbon Monoxide Dehydrogenase 3

C. Techniques 5

(I) K-edge EXAFS 6

(II) L-edge XAS 6

(III) XAS Experiment Set-up 7

(IV) Detection Method 8

(V) Data interpretation 9

(i) EXAFS data analyzing 9

(ii) L-edge data interpretation 9

(1) Chemical Shifts and Branching Ratio 9

(2) X-ray sum rules 9

(VI) Sample Integrity Considerations 9

D. Research Proposal 11

(I) Hydrogenase 11

(i) Model compounds 11

(ii) Proposed hydrogenase samples for XAS 14

(iii) FTIR characterization of sample homogeneity 14

(iv) EXAFS measurements 15

(v) L-edge measurements 16

(II) CO Dehydrogenase 18

(i) Experiments for probing the Acetyl-CoA Synthase Oxidation Site 19

(1) EXAFS measurements 19

(2) L-edge measurements 19

(ii) Experiments for probing the CO oxidation site 20

References
20

I am involved in using the X-ray Absorption Spectroscopic techniques as applied to Ni enzymes -- NiFe hydrogenase and Carbon Monoxide Dehydrogenase.

A. Scientific Questions and Specific Aims

For hydrogenase, CO dehydrogenase/ACS such Ni containing enzymes, there are still questions about:

1. The appropriate description of Ni oxidation states and spin states in different forms,
2. The sites of small molecules binding, and
3. Ni-Fe distances.

The purpose of my proposed research is to help answer these and other questions about the electronic and molecular structure of these Ni enzyme intermediates. And finally get a better understanding of the catalytical mechanism of each enzyme.

B. Biological Systems

Ni was considered to play a specific role in biology after 1975 that the active site of urease contained specifically bound Ni atoms[1]. After that, a number of enzymes have been shown to involve Ni as part of the active site. And these enzymes include: urease, carbon monoxide dehydrogenases (CODHs)/Acetyl-CoA Synthase(ACS), hydrogenase, methylcoenzyme M reductase and recently discovered superoxide dismutases(SODs)[1-4]. Many questions still exist about the role of Ni in catalytic mechanisms: they are essential information such as the nature and geometry of Ni ligands (in certain states), the best description of the Ni oxidation states, exact Ni-Fe distances and even where substrates and inhibitors bind.

(I) Hydrogenase

Hydrogenases catalyze the splitting or synthesis of the hydrogen molecule according to the reaction:

$$H_2 \text{ <--> } 2H^+ + 2e^-$$

These enzymes are the central feature of hydrogen metabolism, which is essential to many microorganisms of great biotechnological interest, such as methanogenic, acetogenic and nitrogen-fixing bacteria. And for the last two decades, hydrogenases have enjoyed renewed interest, mostly in the view of their capacity to store solar energy

as well as produce molecular hydrogen, a clean source of energy[5]. And those hydrogen exhausting bacteria are also the most ancient species during evolution. Understanding the machenism of their hydrogen metabolism can provide us clues to evolution too.

Ni is found in the majority of known hydrogenases, known as NiFe hydrogenase, which contain a single Ni site as well as several different Fe-S clusters and a unique Fe center[5]. The NiFe hydrogenase from D. *gigas* is a heterodimeric periplasmic protein consisting of 28K and 60K subunits and contains two [4Fe-4S] clusters, one [3Fe-4S] cluster and a Ni-Fe center[6]. Recent X-ray crystallographic data on the *D.gigas* hydrogenase reveals a 5-coordinate Ni site, bridged through sulfur ligands to an unusual Fe species[7], which has 1 CO and 2 CN- ligands (Figure 1). The remaining centers are more conventional Fe-S clusters, arranged in a linear fashion to transfer electrons to the NiFe active site.

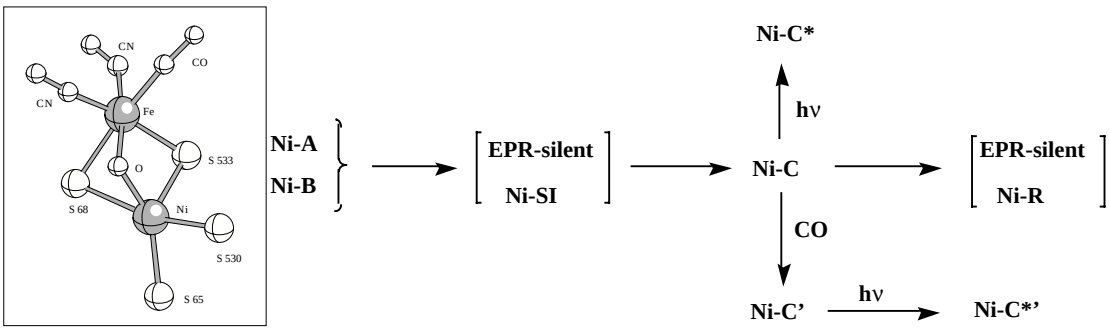

Figure 1. Left: Structure proposed by Volbeda *et al.* [7] for the Ni-Fe site in *D gigas* hydrogenase. Right: Relationships between different forms of hydrogenase throughout the catalytic cycle.

One of the key issues surrounding hydrogenase is the set of oxidation states involved in the catalytic cycle of the enzyme[6]. The redox states of the enzyme were initially defined by their EPR spectral characteristics[8] during EPR-monitored titration, as shown in the scheme in Figure 1. It is now recognized that each state also has a characteristic IR spectrum of CN and CO stretching[9]. For the sequence Ni-B -> Ni-SI -> Ni-C -> Ni-R, Albracht et al. originally proposed oxidation state assignments of Ni(III) -> Ni(II) -> Ni(I) -> Ni(0)[10]. Cammack proposed that Ni remains in the Ni(I) oxidation state and a nearby Fe-S unite becomes reduced[11]. And Moura et al. assigned all of the EPR-active species to Ni(III) and all of the EPR-silence forms as Ni(II)[12, 13]. Maroney and co-works have argued that Ni is unlikely to be redox active and that the redox process is most likely ligand-based[14] from the result of K-edge X-ray spectroscopy.

(II) CO dehydrogenase

Ni-containing carbon monoxide dehydrogenase (CODH) is an important enzyme in the process of carbon fixation. The acetogenic *Clostridium thermoaceticum* (Ct-CODH) converts CO_2 into acetate using the acetyl-CoA pathway of carbon fixation (Figure 2).

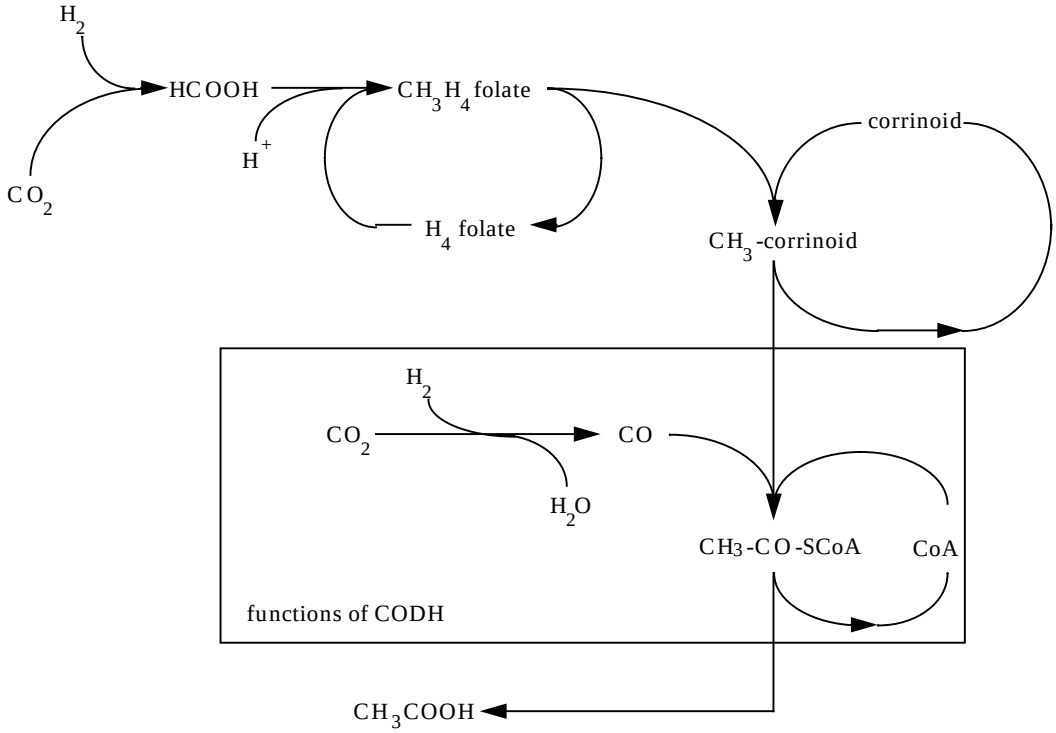

Figure 2. Acetyl-CoA pathway of carbon fixation used by acetogens[15].

Recent electron microscopic[17] studies showed that Ct-CODH is an $(\alpha\beta)_2$ tetramer. There are two Ni, 11-14 Fe and 14 inorganic sulfide per $\alpha\beta$ dimeric unit. Ct-CODH catalyzed acetyl-CoA synthesis and CO oxidation at two distinct sites, Center A and C, respectively[16], both with one Ni bridged to a 4Fe-4S cluster. An additional Fe-S cluster, termed center B composed of 4Fe-4S cluster, may serve as an electron transport site between centers A and C[18].

In the as-isolated state, Ct-CODH exhibits an EPR spectrum resulting mainly from center C, while in the presence of CO, center A develops the S=1/2 NiFeC EPR signal[19]. Upon binding CO, the cluster C undergoes changes in its EPR signal and delivers electrons to cluster B at rates that are catalytically relevant for CO oxidation[16]. Resonance Raman experiments have shown that CO binds to the Fe rather than Ni within the Ni-Fe cluster of center A[16].

Treatment of Ct-CODH with 1,10-phenanthroline(phen) is though to remove Ni from cluster A[20], because the acetyl-CoA activity and the NiFeC signal are both eliminated.

There appears to be heterogeneity among A-cluster Ni species. Only about 0.3Ni/αβ can be removed or reinserted, and the maximum spin integration for the NiFeC signal is about 0.3/αβ [20,21]. These are called 'labile' and 'nonlabile' forms of the A-cluster[20], with only one third of all XOΔH (αβ) dimers containing 'labile' Ni.

Xia et al. have proposed a model involving a Ni^{+}-X^{-}[Fe_4-S_4] assembly with a strong exchange coupling between Ni and one Fe site in the cube[21], and also proposed Ni must present as low spin Ni(II). In the catalytic model for acetyl-CoA activity proposed by Ragasdale[16], the key step is that CO transfer to a metal-bound methyl group. Since the CO binding site and metal oxidation states are unclear, many details are subject to debate.

The geometry and spin-state of Ct-CODH cluster C Ni site remain uncertain. Recent EPR and Mössbauer studies of *R. rubrum* CODH indicate that cluster C contains high spin Ni(II), weakly coupled to an S=1/2 [Fe_4S_4] cluster[22]. EXAFS studies of the *R. Rubrum* CODH indicate that Ni site adopts a five-coordinate geometry[23]. However the spin concentrations are substiochiometric[24], and C-cluster Ni could be distributed between forms with high spin and low spin Ni.

Despite these rather concrete proposals about the Ni spin and oxidation states, most of the Ni in CODH is silent to EPR spectroscopy, and it would be valuable to investigate the metal by an independent technique. And understanding the Ni oxidation states and spin states is an important part in working out the catalytic mechanism. Again, we don't know where the substrate binds. Although there were initial reports that CO binds to the Fe in center A, these have since been retracted. The heterogeneity of center A and C also needs to be explained. What makes one center A 'labile' and another 'nonlabile' ? For both hydrogenase and CO dehydrogenase, fundamental information about electronic and molecular structure is needed before the catalytic mechanism can be described with confidence. And now I will describe why X-ray spectroscopy is a good tool for answering many of these questions. `

C. Techniques

X-ray Absorption Spectroscopy (XAS) has recently become a powerful tool for probing biological samples. XAS is used to probe transitions from atomic core levels. The K-edge absorption represents a transition from the 1s core state, while the L-edge absorption involves a promotion from either the 2s or 2p states, and so on. With the advent of high brightness synchrotron sources, studying the active sites of many metalloproteins, including hydrogenase, nitrogenase, and Photosystem II, has become

possible. I am using the established technique of EXAFS and the rather new developing techniques of L-edge XAS to study Ni-containing metalloproteins.

The techniques of K- and L-edge spectroscopy together give complementary information on both local physical and electronic structure of an absorbing element. The techniques are particularly useful in the study of metalloproteins, in which the active sites are generally the metal containing centers. Information on the local physical structure (within 5 Å of the absorber) of the metals from K-edge spectroscopy, and information on the electronic structure of the metals from L-edge spectroscopy together can be used to help unravel the mechanisms of protein activity.

(I) K-edge EXAFS

Extended X-ray absorption fine structure (EXAFS) is a modulation in the absorption cross section pass an absorption edge. The final states of the electron transition involves interference between outgoing and backscattered photoelectron waves. Depending on whether this interference is constructive or destruction, there is an enhanced or decreased absorption cross section[24].

The equation which describes the EXAFS oscillations as a function of k for an absorbing atom a surrounded by N backscattering atoms b is,

$$\chi(k) = \sum_{b=1}^{N} f_b(k) e^{-2\sigma^2 k^2} \sin[2kR + \Phi_a(k) + \Phi_b(k) - \pi]$$

where $k = [8\pi^2 m_e(E-E0)/h^2]^{1/2}$ is the photoelectron wavevector, Φ_a and Φ_b represent the phase shift the electron experiences as it travels through the potentials of the absorbing and backscattering atoms, R is the distance of each backscatterer from the absorber, Φ_b represents the backscattering amplitude function, and $\exp[-2(\sigma k)^2]$ is often referred to as the Debye-Waller factor.

Each absorber-neighbor pair produces an oscillation in the absorption above the absorption edge, and is represented by a sinusoid in the EXAFS equation. Because the phase shift and backscattering amplitude functions are energy-dependent, the oscillations are not exact periodic functions of k. They are, however, unique to each absorber-backscatter interaction, which allows determination of the type of each backscatterer. The frequency of modulation can be used to determine interatomic distances with an accuracy of 0.02Å derivation, while the amplitude and phase can be used to extract the numbers and elemental types of neighbors, with the accuracy of 20%[24]. EXAFS has become an almost routine technique in bioinorganic structure determination.

(II) L-edge XAS

L-edges result from transitions between the L shell of an atom and higher unoccupied levels, which is subdivided into L_1, which involves the 2s electrons, L_2 and L_3 edges, which come respectively from spin-orbital splitting of the $2p^5$ hole into $2p_{1/2}$ and $2p_{3/2}$ final states. For the first row transition metals, the final state of the L_2 and L_3 edges is the valence shell which makes this technique very sensitive to both the ligand environment and the metal oxidation states. And coulomb and exchange interactions between the 3d-3d electrons and the 2p-3d electrons give rise to the multiplet structure in the L-edge, which can then be used to investigate the metal oxidation and spin states.

What makes L-edge spectra particularly important in study of structure and function of metalloproteins lies in the fact that metal at the protein active site often undergoes oxidation states, spin states or symmetry changes during the catalytic cycle.

L-edge is elemental selectivity - one can examine one particular element at a time. It gives better energy resolution as compared to K-edge[26]. As L-edge is lower in energy than K edge (Ni L_3 edge 852.7 eV, K edge 8333 eV), the core hole lifetime is increased ($E\ t = h/2\pi$), and result in narrower linewidth (transition metal K-edge have linewidths of 1-2 eV, while the intrinsic linewidths of L-edge are narrowed down to 300-700 meV)[26]. And other factors, such as favorable selection rules, multiplet splittings and strong magnetic circular dichroism make L-edge X-ray spectroscopy a good technique to our biological system.

(III) XAS Experiment Set-up

EXAFS measurement can be done in the air or He atmosphere. I used beamline 7-3 at SSRL, with the standard EXAFS setup, using Liquid He flow through cryostat and a Canberra 13 element Ge detector. However for L-edge spectroscopy, things are more complicated. Because the L-edge is lower in energy (500 - 1000 eV) than the corresponding K-edge transitions (5000 - 10000 eV),there is a much larger absorption cross-section. For example, at Ni L-edge the 1/e path length for an X-ray in water is only 1.0 micron, and the path length in air less than 4 cm. So my experiment on L-edge requires to work in a vacuum chamber. The experimental setup for the L-edge experiment in shown in Figure 3.

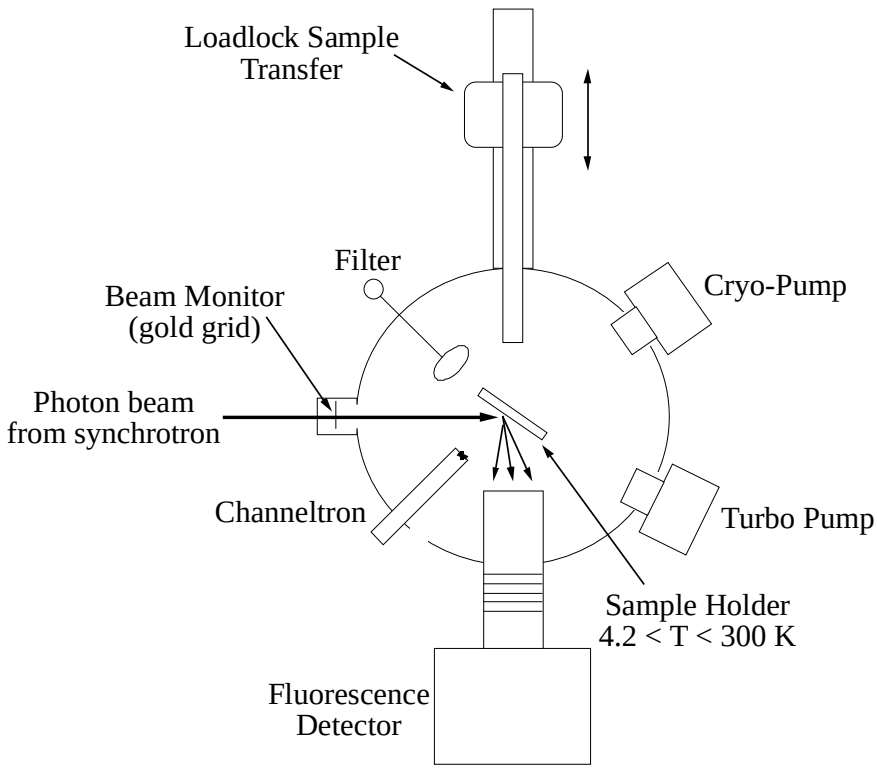

Figure 3. Experimental setup for soft x-ray absorption.

Turbo and cryopumps are used to maintain a vacuum of better than 10^{-9} Torr, and the vacuum chamber is attached to the beamline without the use of intervening windows, which is necessary (1) to avoid condensation of air or water on cold sample and (2) to allow connection to UHV beamline. The incident photon flux is obtained by measuring the current induced in a gold grid placed in the beam path.

(IV) Detection Methods

Direct measurement of an absorption spectrum consists of measuring the incident and transmitted X-ray flux, I_0 and I respectively, and deriving the absorption coefficient $\mu t = \ln (I_0/I)$ as a function of X-ray energy. However for dilute Ni protein samples, it is difficult to observe a small signal change in the presence of a large background signal from water and protein absorption. Also very small instrumentally derived fluctuation in the background can't be distinguished from signal. To avoid artifacts and achieve better sensitivity, 'secondary' detection methods are used. In my experiment, I used fluorescence signal detection, which makes use of the fact that an inner shell hole may relax by undergoing a radioactive transition from a higher energy occupied shell. The sensitivity of this technique for hard X-ray EXAFS has long been recognized[27]. The uncertainty of a transmission experiment scales as $1/\mu t$, which in fluorescence detection,

the uncertainty scales as $(1/\mu t)^{1/2}$[27]. Recently, fluorescence detection applications in L-edge metalloprotein spectroscopy have been developed[28].

(V) Data Interpretation

(i)EXAFS analyzing

I am using EXAFSPAK programs, developed by Dr. G. N. George of SSRL, to analyze the EXAFS spectra. Based on the theoretical calculations, the program includes a degree of automation, an efficient curve-fitting algorithm using analytically calculated derivatives and other features.

(ii) L-edge spectra interpretation

There are many features to characterize the elements from X-ray spectra. However since we are dealing with more covalently bound Ni site in the protein, the single configuration model starts to break down and useful features such as multiplet splittings become less pronounced and less useful[24]. Fortunately, there are other features of spectra which can help.

(1) Chemical Shifts and Branching Ratio

Absorption edges shift to higher energies with increasing oxidation states. This can be easily explained as a reduction in the screening of the nucleus by valence electrons, hence an increase in the apparent nuclear charge. Another approach is to look at the correlation between the L_3 Centroid energy and the branching ratio[24]. The branching ratio is the ratio of the integrated L_3 intensity to the total L_3 + L_2 intensity. This ratio changes with spin states with small value for low spin and large value for high spin[24]. Thus this methods provide an independent way of characterize Ni spin states in enzymes.

(2) X-ray sum rules

This methods uses the idea to deduce the distribution of electrons in a compounds by measuring the presence of 'holes'. The total cross section sum rule for L-edges says that the intensity integrated over the L_3 and L_2 'white lines' is proportional to the number of empty states. Since the 2p -> 3d transitions is dominant in L-edge transition, the metal 3d vacancies can be deduced.

(VI) Sample Integrity Consideration -- FT-IR characterization

For hydrogenase, although some states of the enzyme can be characterized for homogeneity by EPR spectroscopy, other forms such as silent intermediate (Ni-SI) and fully reduced (Ni-R) are EPR-silent with respect to Ni. We would have to use other program to characterize samples before X-ray spectroscopy by FT-IR analysis.

Fourier transform infrared studies (FTIR) of NiFe hydrogenase from both *C.vinosum* and *D.gigas* revealed the presence of three absorption bands in 2100-1900 cm^{-1}[29, 30]. These bands are sensitive to the redox states of the enzymes and the frequency shifts due to the redox states changes. Happe et al. [31] have identified the groups responsible for the IR bands in *C. vinosum* hydrogenase, both chemically and by isotopic labeling, as two CN^{-1} and one CO, which are most likely the three diatomic ligands of the active site Fe observed in crystallographic analysis of the *D. gigas* enzyme[7]. Therefore, the shift of these bands can be thought of as a sensitive marker for the Ni-Fe site redox status.

I have done some FT-IR measurement on D. gigas hydrogenase using dehydrated film on a sapphire plate. The films of the *D.gigas* enzyme show essentially single CO stretching frequency at the same frequency reported for solution spectroscopy of Ni-A. Furthermore, the films maintain the chemical changes performed in solution, as evidenced by the change in peak position. The figure below showed the preliminary result of FT-IR spectra of *D.gigas* hydrogenase.

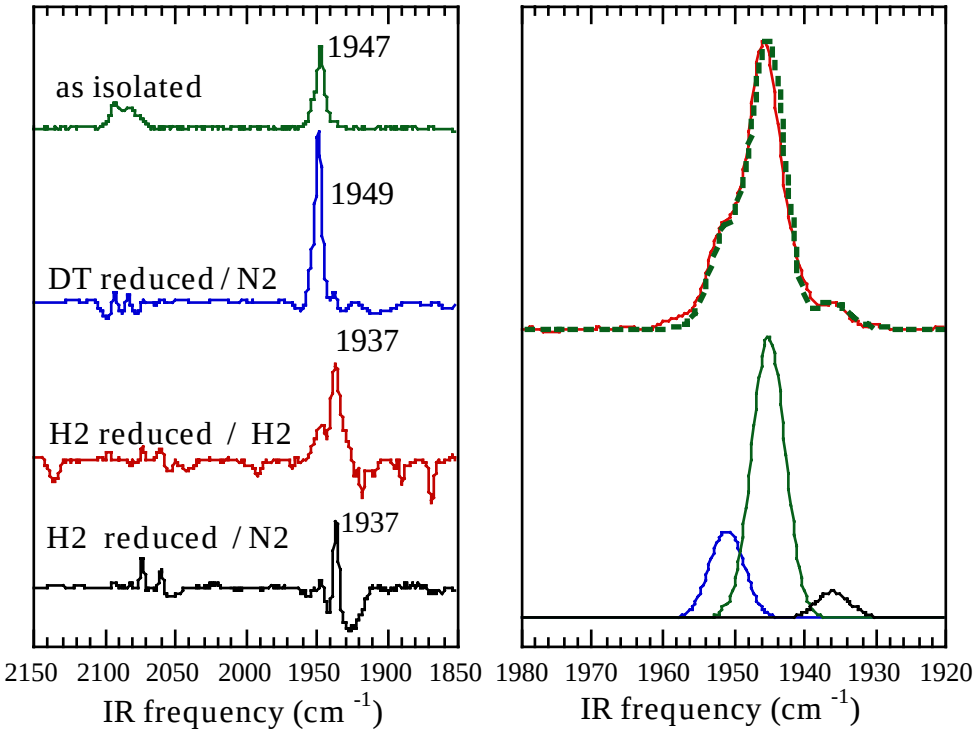

Figure 4. (Left) The FT-IR spectra of different redox states of *D.gigas* obtained on dehydrated films. (Right) The peak-fitting analysis of *D.gigas* H_2ase films. Top – solid line: experimental data, dotted line: simulated spectrum, bottom - individual components used in the simulation.

D. Research Proposal

Much of the information one would like to obtain about a particular metalloenzyme active site can be summarized in terms of its electronic and molecular structures and how these changes in their characteristics lead to the desired enzyme activity.

Crystallography or more conventional types of spectroscopy such as EPR and ENDOR, can't supply all of the necessary information needed to fully understand the questions of these Ni enzymes. My proposal is applying K- and L- edge x-ray spectroscopy, with particular attention paid to obtaining homogeneous well-characterized samples with the help of our biochemist collaborators. When homogeneous Ni sites are biochemically impossible to obtain, we will at least quantitative the amounts of different species. Spectroscopic sample characterization will be done by EPR and FT-IR on the same sample used for X-ray measurements.

(I) Hydrogenase

The specific goals of the hydrogenase experiments are (1) to measure the number of d-holes on Ni for different enzyme redox states. (2) to measure the spin and orbital angular momentum of the Ni sites in certain paramagnetic forms, and (3) to monitor the Ni-Fe and Ni-ligand distances for different redox states and CO-inhibited forms by EXAFS. The first two problems are being pursued by our other colleagues in our group. I am proposed to do the Ni EXAFS measurements on different redox states of Ni hydrogenase to monitor the geometry and electronic state changes during the catalytic circle and also participate in the L-edge measurements.

(i) Some model compounds preliminary results

We need appropriate model compounds to correlate edge and EXAFS analysis with oxidation states, ligand type and coordination geometry. Such comparative approach limits us to geometric and oxidation states exhibited by the available model compounds, a limitation that is not favored by the metalloenzyme active sites.

Several kinds of model compounds were chosen at the mean time, which include the Ni-dithiolene compounds with different Ni oxidation states, and Ni-Fe compounds which resembled the Ni-Fe cluster inside of hydrogenases and CODHs. I did the EXAFS measurement on these compounds. The compounds I used can be generally written as $Ni[S_2C_2R_2]_2^{0,+1,+2}$, and the structure is shown as:

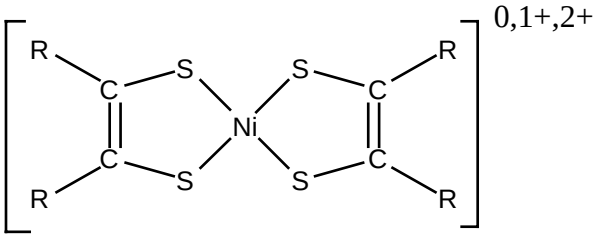

Ni oxidation states can be monitored to be IV, III and II respectively, and R = CF_3, CN and Ph_2. The EXAFS spectrum and fitting of the peak is shown as the following. When analyzing the data, I used only the first shell(4S) to fit the main peak, which can provide the ligand information of the Ni environment inside of hydrogenase.

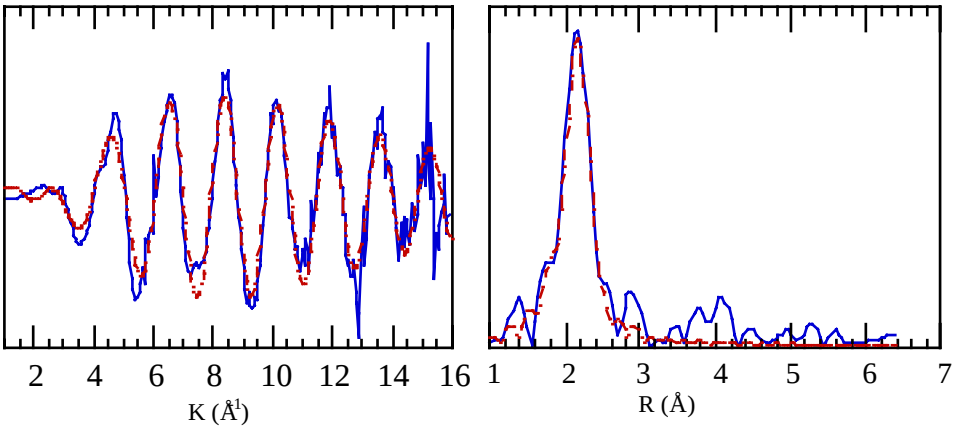

Figure 5 . (Left) The EXAFS modulations(solid line) and best fit (dotted line) using only first shell 4S of compound Ni(IV)[$S_2C_32(CF_3)_2]_2$. (Right) The Fourier transformed EXAFS(solid line) and best fit(dotted line) using only first shell 4S of the compound Ni(IV)[S_2C_2 $(CF_3)_2]_2$. The Ni-S distance is 2.12Å.

The EXAFS analysis and comparation of these Ni-dithiolene compounds give the following table:

R	CF_3		CN		Ph_2	
Parameters	**Ni-S (Å)**	σ^2	**Ni-S (Å)**	σ^2	**Ni-S (Å)**	σ^2
Ni (II)	**2.16**	**0.002**	**2.15**	**0.002**	**N/A**	**N/A**
Ni (III)	**2.14**	**0.002**	**2.18**	**0.002**	**2.14**	**0.002**
Ni (IV)	**2.12**	**0.002**	**N/A**	**N/A**	**2.12**	**0.001**

Table 1. Fits of first coordination sphere Ni EXAFS from model compounds.

The analysis of the EXAFS data doesn't reveal any significant change in Ni-ligand bond length of the Ni-dithiolene as a function of Redox State of the enzyme. The Ni-S distance obtained from the fits are essentially identical at 2.14 ± 0.03 Å. In contrast, the

bond lengths reported for an isoleptic pair of Ni (III/II) model $Ni(pdtc)^{-/2-}$, exhibit an increase of 0.14Å in the average Ni-S distance[32].

According to our understanding, the charge on the metal center is determined by a combination of two factors: the oxidation state of the metal and the ability of the ligands to reduced the positive charge on the metal through covalent interactions. The increase of metal oxidation states may decrease the bond distance, however it is still possible that the covalently bonded ligand may act as electron donor to the metal to reduce the positive charge on the metal, so that the bond distance doesn't change obviously upon oxidation. The Ni in the hydrogenase might be similar to such situation.

Another model compound I used is a Ni-Fe complex which resemble the Ni site in hydrogenase and CO dehydrogenase. The compound is synthesed as $(Bu_4N)[FeS_4TrisNiS_2N_2]$, Where Tris= 1,3,5-Triethyl-2,4,6-tris(3-sulfanylindolyl-1-methyl)benzene. And the structure we are interested in is drawn as below:

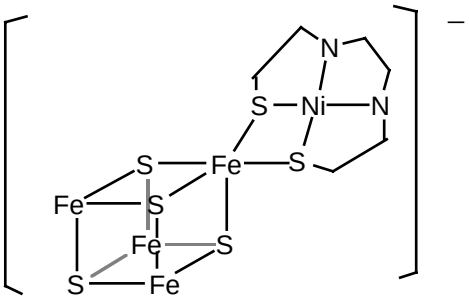

The EXAFS data and fits are shown in figure 6. After I fitted the first two shell as 2S and 2N, I used search profile program to search for the best Ni-Fe distance and get the minimum point at R=2.44 Å.

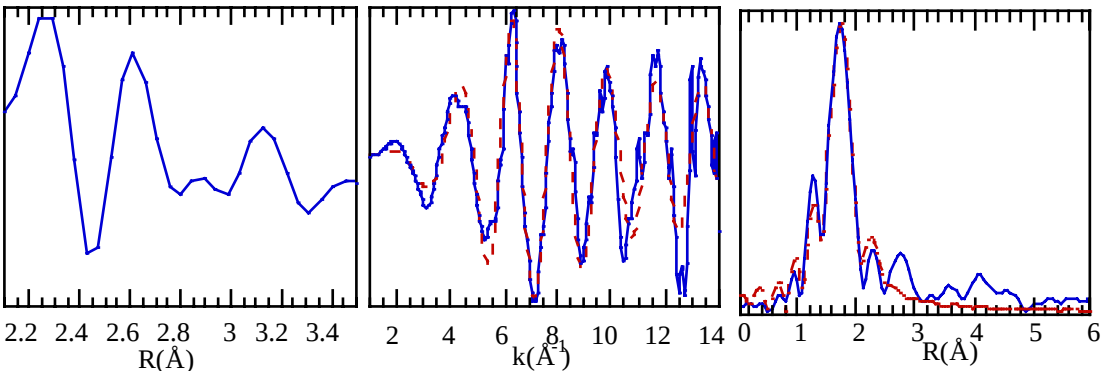

Figure 6. (Left) the search profile of Ni-Fe distance. (Middle) EXAFS modulation(solid line) and best fit(dotted line) of Ni-Fe compounds. (Right) Fourier transformed EXAFS(solid line) and its best fit(dotted line) of Ni-Fe compound. The fitting parameters are Ni-S R=2.15Å, σ^2=0.0004; Ni-N R= 1.88 Å, σ^2=0.0094; Ni-Fe R=2.45, σ^2=0.0038.

(ii) Proposed Hydrogenase samples for X-ray analysis

In hydrogenase, some forms are easier to prepare as homogeneous samples when using enzyme from one organism instead of another. For example, form A comes naturally from the as-isolated D. gigas preps, while it has not been observed for *P. furiosus* enzyme.

The sample will be initially prepared as partially dehydrated thick film on a IR transmissive substrate, in this case I will use polypropylene which is good for EXAFS measurement also. The preparation will be done inside an inert atmosphere glove box, or in CO- or H2-filled Schlenk tubes as necessary.

Form A -- I will use *D.gigas* H2ase, one of the classical forms of hydrogenase with which the crystallography has been done.

Form B - 'inactive' and 'active' -- D. *desulfuricans* H_2ase is chosen. The enzyme is primarily in the 'inactive' from B as isolated. It can be reduce and reoxidized to obtain so-called 'active' form by 'reductive activation[33]. And I am expecting to get some clue about the nature of reductive activation step by comparing the spectra of these two forms.

Form SI (silent intermediate) -- D. gigas and D. *baculatus* are chosen for this kind of form. *D.gigas* enzyme can be reduced and then reoxidized back to a potential that optimizes form SI while D. *baculatus* enzyme is primarily SI as-isolated.

Form C -- D. gigas H_2ase is good for this form. This S=1/2 species is optimized at potentials between those for SI and Form R enzyme. The protein samples can be monitor dyes to optimize the conversion to form C and then quantitative the amount of other species by FT-IR.

Form R -- This form can be obtained from *D.gigas*, D. *baculatus* and *P.furiosus*. The samples can be obtained by prolonged exposure of enzyme solution to purified H_2, followed by film preparation under a H_2 atmosphere.

(iii) FT-IR characterization of sample homogeneity

Since the 2100-1900 cm^{-1} IR bands of hydrogenase[29, 30] are sensitive to the redox states of the enzymes and the frequencies shifts due to the redox states changes, the shift of these bands can be thought of as a sensitive marker for the Ni-Fe site redox status.

I will run FT-IR measurement on the proteins before EXAFS measurement to monitor the sample integrity.

The figure below is the simulation of the strong band around 1950 cm^{-1}. It is shown that in *D. gigas* H_2ase, the Diothiolene reduced and H_2 reduced enzymes have a high integrity. The FT-IR of *P. furiosus* enzyme has never been reported. And my results showed the samples are less homogeneous when prepared. Working with our group collaborator in Prof. Adams group, we hope to get more integrity H_2ase samples for the X-ray measurements.

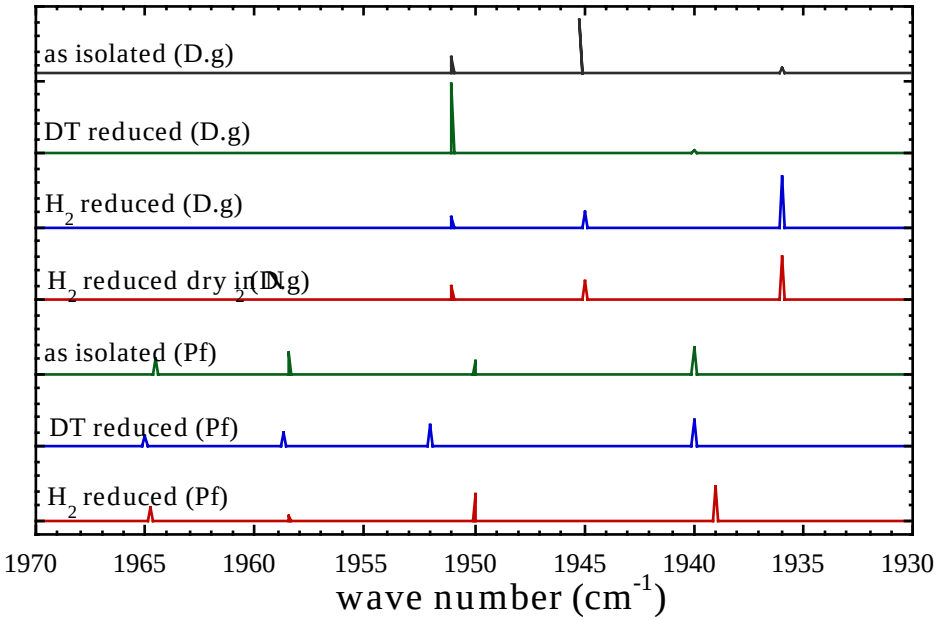

Figure 7 . The relative intensity of the simulation of the 1950 cm^{-1} band of different forms of *D.gigas* and *P.furiosus* H2ase.

(iv) EXAFS measurements

The EXAFS of many different hydrogenase preparations has already been reported[13, 34-37]. However the Ni-ligand and Ni-Fe distances didn't been well defined. Maroney et. al. [36, 13] proposed the Ni site is trigonal-bypyramidal. And Gu et al. [37] stated that the Ni environment is consistent to the recent crystallography data[7], however it is difficult to distinguish Ni-S from Ni-Fe scattering at the distance 2.4 - 2.9 Å. There are several reasons for this problem. First, the samples measured are not in a homogeneous state. Analysis of such EXAFS data can only yield an average environment that might have significant disorder. Second, most the EXAFS data is only useful out to 12.5 $Å^{-1}$. This upper limit was due to the presence of trance amount of Cu in the samples(since Cu K edge is 8979 eV). If we can successfully take data out to 16 $Å^{-1}$, the Ni-Fe distance should be unambiguous.

Therefore, for my future research, my concerning is (1) I will use the films instead of frozen solution samples previously examined since films are significantly (~ 5-fold) more concentrated. (2) I am planing to use 30-element Ge detector instead of 13-element detector to get better resolution and 10-fold higher throughout. (3) Any traces of adventitious Cu should be removed from the sample, using dialysis against EDTA buffers and/or recrystallization of the protein. (4) I would also try some single crystal EXAFS on the hydrogenase. The crystal will be provided by our collaborator.

(v) L-edge Spectroscopy

One of the key problems concerning NiFe hydrogenase is the Ni oxidation states involved in the catalytical cycle. From former EPR spectroscopy, people have proposed several possible Ni oxidation assignments during catalytical cycle of the reaction [8,10-13]. However, these assignments are based on the redox states of the system, rather than on any compelling spectroscopy evidence. And since there are some EPR silent species during the redox titration, EPR along couldn't provide sufficient evidences for the Ni oxidation states.

Previous K-edge XANES studies of NiFe hydrogenases have not provided a consistent explanation of the Ni electronic structure either. Shifts in the *D. gigas* hydrogenase K-edge were interpreted to indicate that Ni is reduced from Ni(III) in the native state to Ni(II) upon reduction by hydrogen[38]. However, K-edge studies on *Thiocapsa roseopersicina* hydrogenase in several redox states showed no significant shifts in nickel edge position, suggesting a non-Ni based redox chemistry[14]. Ni K-edge XAS studies of the oxidized and reduced forms of several hydrogenases indicate at most a one-electron reduction of the metal centers, but no specific oxidation states were proposed[37]. Since the progress[24,26] as discussed above has made L-edge X-ray absorption a useful method which is complementary to K-edge XANES and EPR, we have begun a systematic evaluation of Ni enzymes by this technique.

As stated above, model compounds have played an important role in developing quantitative X-ray spectroscopy. For soft X-ray spectroscopy, analysis of well defined model compounds helps build confidence that the simulation and sum rule analyses are giving sensible results. From our groups' previous work on many Ni compounds, the branching ratios correlation diagram (Figure 8) and sum rule intensity diagram (Figure 9) have been made and can be used to quantitatize the Ni spin and oxidation states.

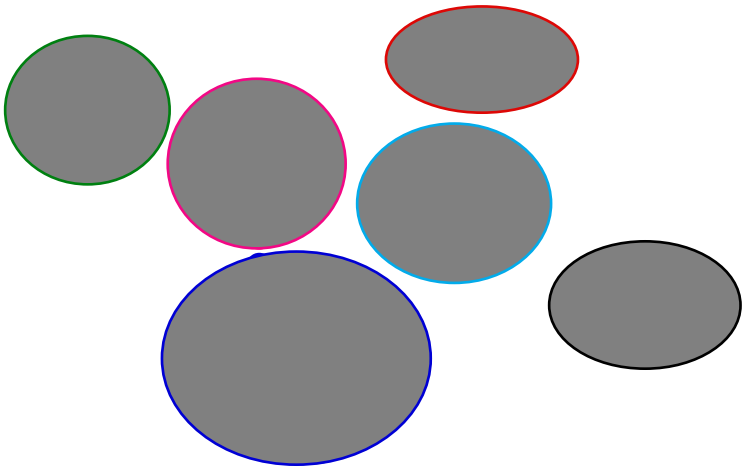

-

Figure 8. L 3 centriod position and branching ratio For different Ni compounds.

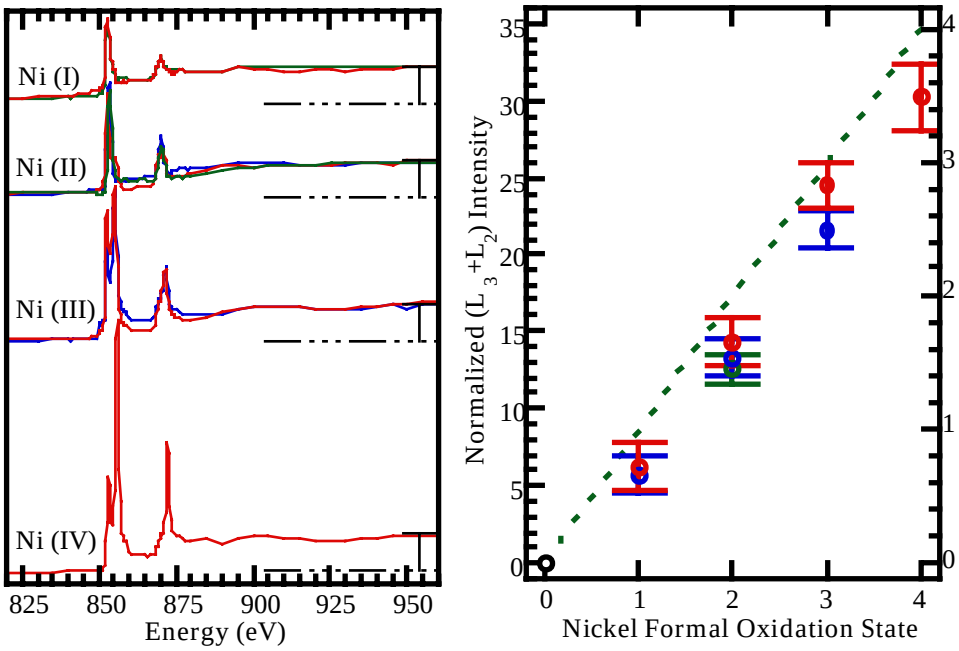

Figure 9. (Left) Comparison of normalized L-edges for (top to bottom) Ni(I), Ni(II), Ni(III) and Ni(IV). (Right) The integrated intensity of the L-edge resonance features as a function of formal oxidation state. The dotted line represents our best estimate for the purely ionic limit.

The L-edge measurement on Ni hydrogenase is being pursued by our group. And the samples we have been looked at are from *D. gigas*[39] (Figure 10). From the multiplet structure simulation, the features of the as-isolated enzyme spectra are best simulated as

high spin Ni(II), it isn't accord with the previous magnetic susceptibility data[40], which showed that Ni is diamagnetic. And it raises the problem if Ni spin states changes under L-edge experimental condition. So further work is needed with parallel FT-IR studies. The L-edge branching ratio and sum rules are quite a good tool to interpret the L-edge spectroscopy, however the edge jump which is used for normalization is hard to measure for hydrogenase samples. Other methods to normalize the edge intensity is being tested. One of which is to doped appropriate heavy metals into the protein sample and use their intensity as normalization.

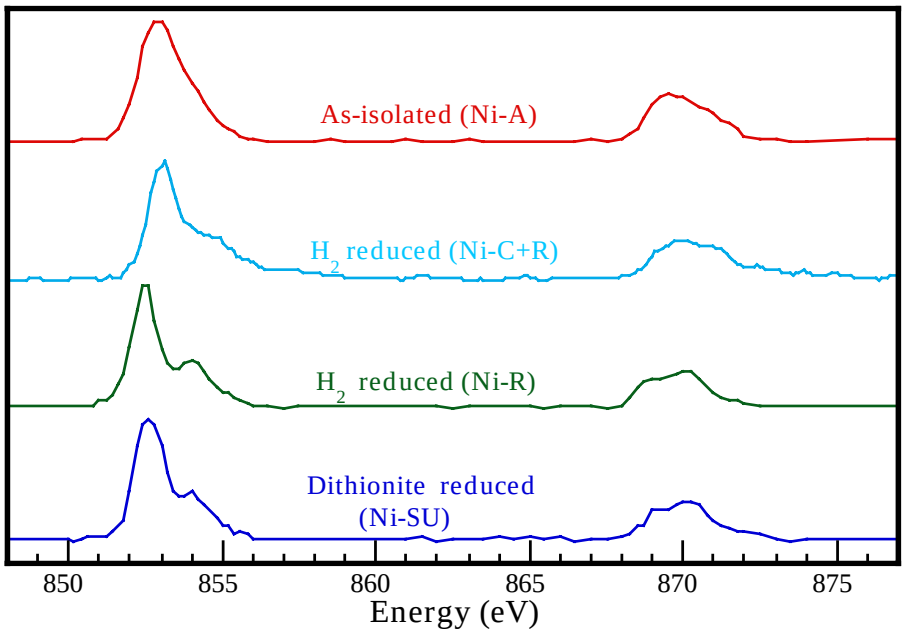

Figure 10. Ni L-edge spectra for D. gigas (from top to bottom) Ni-A, Ni-C+R, Ni-R and Ni-SU.

We propose to do the L-edge on other hydrogenases from other bacteria. And combined with the K-edge EXAFS from different forms we can get inside of the geometry, redox states and spin states changes during the catalytical cycle.

(II) CO dehydrogenase

For CO dehydrogenase, my proposed goals are (1) to use L-edge spectroscopy to address the oxidation state and spin state of the various Ni species and (2) to use EXAFS to better define Ni-Fe distances.

As discussed in above in background, a major problem for Ct-CODH experiments is that there are two types of Ni cluster, center A and center C, and these in turn are divided into 'labile' and 'nonlabile' forms of center A and two forms of center C with different redox states. A protein with only C-cluster comes from naturally from *R.rubrum*. The

isolated A-cluster can be obtained by separating the a subunit from the intact protein from *C. thermoaceticum*.

(i) Experiments for probing the Acetyl-CoA Synthase Oxidation Site

(1) K- edge EXAFS

Previous spectroscopy work has given us some evidence of the structure at the active sites. Mössbauer and ENDOR studies are consistent with a Ni bridged to an 4Fe-4S cluster structure for center A[41,42]. Resonance Raman experiments have shown that CO binds to the Fe rather than Ni within the Ni-Fe cluster of center A[43]. Previous Ni EXAFS studies of Ct-CODH have examined the enzyme in the as-isolated or reduced states, and have shown the Ni to be ligated by both S and O/N atoms[44-45]. Our group had done the EXAFS on the Ct-CODH with the as-isolated and CO treated forms[46]. From these studies, it was found that Ni is ligated to 2 S and 2 N/O in a distorted geometry, and the Ni-Fe distance are around 2.7 - 2.9 Å. However since the problem we mentioned before when discussing hydrogenase EXAFS, the Ni-Fe distances are poorly defined. Furthermore, since Ct-CODH has two subunites and two Ni sites at Center A and Center C respectively, the EXAFS analysis could not separate the these different Ni sites.

Now my proposal is to use the separated subunit which only contain one Ni center. With the same experimental setup for hydrogenase EXAFS. The protein samples I propose to use are oxidized, methylated and carbonylated forms of Ct-CODH.

From the EXAFS analysis, I expect to get such information:

1.To get better resolved data to extract the Ni-Fe distances of Center A.

2. If we treated the sample with phen, we could get the 'non-labile' form of the center A. We can see if there is any differences in geometry with the non-labile form and labile form.

3. Can we see a Ni-CO interaction in the carbonylated A-cluster? - in the absence of the C-cluster, we have a good chance of seeing the Ni-CO interaction(if there is one) in the EXAFS.

4. Can we see a Ni-C bond in the EXAFS of the methylated form?

(2) L-edge measurement

From EPR and Mössbauer spectra of CO-reduced species, Xia and coworkers[21] proposed there is a strong exchange coupling between Ni and Fe site and they also concluded Ni must be present as low-spin Ni(II). However since most of the Ni in CODH

is silent to EPR spectroscopy, we need other independent method. L-edge spectra are sensitive to oxidation and spin states changes of the absorbing element.

The previous L-edge measurement of our group has got such results[46], that is as-isolated CODH samples contain mainly low-spin Ni(II), while the CO-treated form contains Ni(I). However, since there are two Ni sites in Ct-CODH, and Center A contains non-labile and labile Ni. We don't know which one is which, and whether there are any differences between labile and non-labile Ni sites.

So I propose to use L-edge to investigate the Ni oxidation and spin states in different forms of isolated Center A, non-labile, labile forms, oxidized, methylated and carbonylated forms. And I expect to see that:

1. Is the Ni in the carbonylated form a Ni(I) complex or a high-spin Ni(II) complex? - Better L-edge spectra and sum rule analysis will allow us to make a unambiguous conclusion.

2. What are the differences between Ni ions in 'labile' and 'nonlabile' A-clusters? If there is a change in spin state.

(ii) Experiments for probing the CO oxidation site

The geometry and spin-state of Ct-CODH Center C Ni site remains uncertain. A distorted tetrahedral or 5-coordinate geometry was inferred from K-edge spectra[45]. EXAFS studies of *R. Rubrum* CODH indicate that Ni site adopts a five-coordinate geometry[23]. Our previous EXAFS[46] studies of Ct-CODH couldn't distinguish the Center C from Center A.

Our group collaborator, Ragsdale group can prepare an isolated CO oxidation subunit from the *C. thermoaceticum* CODH that contains a single C-type nickel iron-sulfur cluster. They will poise this subunit in several key states of protein(so called C_{ox}, C_{red1} and C_{red2} states) for L-edge and EXAFS analysis. And other type of samples from *R.ruburm* enzyme will also be investigated. The questions I will try to address are:

1. By using L-edge measurement, we can see if there is a Ni oxidation between C_{ox} and C_{red1}?

2. From L-edge spectra and sum rule analysis of homogeneous samples, we would like to know if the Ni in the C_{red2} form a Ni(I) complex or a low-spin Ni(II) complex.

3. From EXAFS and L-edge experiments, I would like to see if there are differences between Ni ions in reducible and nonreducible C-clusters.

References:

1. Dixon, N.E. Gazzola, D. et. al., *J.Am.Chem. Soc.* 97: 4131 (1975)

2. Lancaster, J. R. VCH Publishers, NY (1988)
3. Hausinger, R.P. Plenum, NY (1993)
4. Youn, H. D., Kim, E. J., et. al., *Biochemical Journal*, 318, 889-896 (1996)
5. Albracht, S. P. J., *Biochim. Biophys. Acta*, 1188, 167-204 (1994)
6. Huynh, B. H. et. al., *Biol. Chem*. 262, 795-800 (1987)
7. Volbeda, A., Charon, M. H., et. al., *Nature* 373, 580-587 (1995)
8. Cammack, R. Fernandez, V. M., Hatchikian, E. C., *Methods Enzymol* 243, 43 (1994)
9. Volbeda, A., Fernandez, V. M., de Lacey A.L. et. al., *J. Am. Chem. Soc*. 118, 12989-12996 (1996)
10. van der Zwaan, J. W., Albracht, S.P.J., et. al., *FEBS Letters*, 179, 271 (1985)
11. Cammack, R., Rao, K. K., et. al., *Biochimie*, 68, 93 (1986)
12. Moura, J. J. G., Teixeira, M., et al., *The Bioinorganic Chemistry of Nickel*, VCH Publishers, NY (1988)
13. Moura, J. J. G., et al., *Pure. Appl. Chem*. 61, 915 (1989)
14. Bagyinka, C., Moroney, M. J., et al., *J. Am. Chem. Soc*., 115, 3576-3585 (1993)
15. Brock, T. D. "Evolutionary Relationships of the Autotrophic Bacteria," in *Autotrophic Bacteria*; Schlegel, H. G. and Bowien, B. ed.; Science Tech Publishers: Madison, WI, 1989, pp 499.
16. Ragsdale, S. W. and Kumar, M., *Chem. Rev*., 96, 2515-2539 (1996)
17. Xia, J. Q.; Sinclair, J. F., et al., *Biochemistry*, 35, 1965-1971(1996)
18. Kumar, M.; Lu, W.-P.; Liu, L. F.; Ragsdale, S. W. *J. Am. Chem. Soc. 115*, 11646-11647 (1993)
19. Gorst, C. M.; Ragsdale, S. W. *J. Biol. Chem.* 266, 20687(1991)
20. Shin, W. and Lindahl, P.A., *J.Am. Chem. Soc*., 114, 9718- 9719 (1992)
21. Xia, J. Q., Ju, Z. G., et al., *J. Am. Chem. Soc*., 119, 8301-8312(1997)
22. Hu, Z. G., Lindahl, P. A., et al., *J. Am. Chem. Soc.*, 118, 830-845 (1996)
23. Tan, G. O., Ensign, S. A., et al., *PNAS*, 89, 4427-4431(1992)
24. Cramer, S. P., Wang, H. X., et al, *"Spectroscopic Methods in Bioinorganic Chemistry*" ACS Symposium Series (1997)
25. Stern, E. A. in *X-Ray Absorption: Applications and Techniques of EXAFS, SEXAFS, and XANES*; Koningsberger, D. C. and Prins, R. ed.; John Wiley & Sons: New York, 1988, pp 1
26. Krause, M. O. and Oliver, J. H., *J. Chem. Phys. Ref. Data*, 8, 329-337 (1979)
27. Jaclevic, J., Kirby, J. A., et al., *Sol. State Comm*. 23, 679-690 (1977)
28. Cramer, S. P., Chen, J., et al., *Nucl. Inst. Meth. A*., 319, 285-228 (1992)
29. Bagley, K. A., Woodruff, W. H., et al., *Biochemistry*, 34, 5527-5535 (1995)

30. de Larcey, A. L., Hatchikian, E. C., et al., *J. Am. Chem. Soc*., 119, 7181-7189 (1997)
31. Happe, P. R., Bagley, K. A., *Nature*, 385, 126 (1997)
32. Kruger, H.J., Holm, R. H. *J. Am. Chem. Soc*. 1990, 112, 2955-2963.
33. Bagley, K. A., Vangarderen, C. J., et al., *Biochemistry*, 33, 9229- 9236 (1994)
34. Whitehead, J. P., Colpas, G. J., et al., *J. Am. Chem. Soc*. 113, 6288- 6299 (1991)
35. Maroney, M. J., Colpas, G. J., et al., *J. Am. Chem. Soc*. 113, 3962- 3972 (1991)
36. Whitehead, J. P., Maroney, M. J., *J. Am. Chem. Soc*. 115, 5629- 5635 (1992)
37. Gu, Z., Dong, J., Maroney, M. J., *J. Am. Chem. Soc*. 118, 11155- 11165 (1996)
38. Scott, R. A., Moura, I., et al., *J. Am. Chem. Sco*. 106, 6864 (1988)
39. Cramer, S. P., Peng, G., et al., *Inorg. Chem*. 34, 2501- 2504 (1995)
40. Wang, C. P., Franco, R., et al., *J. Biol. Chem*. 267, 7378 (1992)
41. Lindahl, P. A., Ragsdale, S. W., et al., *J. Biol. Chem*. 265, 3880 (1990)
42. Fan, C. L., Gorst, C. M., Ragsdale, S. W., et al., *Biochem*. 30, 431 (1991)
43. Qiu, D., Ragsdale, S. W., et al., *Science*, 264, 817 (1994)
44. Bastian, N. R., Deikert, G., et al., *J. Am. Chem. Soc*. 110, 5581- 5583 (1988)
45. Xia, J. Q., Dong, J., Lidahl, P. A. *J. Am. Chem. Sco.* 117, 7065 - (1995)
46. Ralson, Corie *Ph.D thesis*, 1997